NREL/CP-5400-63091. Posted with permission.
Presented at the SAE 2015 World Congress & Exhibition, 21–23 April 2015, Detroit, Michigan.

2015-01-0763
Published 04/14/2015

doi:10.4271/2015-01-0763
saefuel.saejournals.org

Heat of Vaporization Measurements for Ethanol Blends Up to 50 Volume Percent in Several Hydrocarbon Blendstocks and Implications for Knock in SI Engines

Gina M. Chupka, Earl Christensen, Lisa Fouts, Teresa L. Alleman, Matthew A. Ratcliff, and Robert L. McCormick
National Renewable Energy Laboratory

ABSTRACT

The objective of this work was to measure knock resistance metrics for ethanol-hydrocarbon blends with a primary focus on development of methods to measure the heat of vaporization (HOV). Blends of ethanol at 10 to 50 volume percent were prepared with three gasoline blendstocks and a natural gasoline. Performance properties and composition of the blendstocks and blends were measured, including research octane number (RON), motor octane number (MON), net heating value, density, distillation curve, and vapor pressure. RON increases upon blending ethanol but with diminishing returns above about 30 vol%. Above 30% to 40% ethanol the curves flatten and converge at a RON of about 103 to 105, even for the much lower RON NG blendstock. Octane sensitivity (S = RON - MON) also increases upon ethanol blending. Gasoline blendstocks with nearly identical S can show significantly different sensitivities when blended with ethanol. HOV was estimated from a detailed hydrocarbon analysis (DHA) as well as using a differential scanning calorimetry/thermogravimetric analysis (DSC/TGA) method. The DHA method allows relatively straight-forward estimation of fuel composition and temperature effects, and errors are estimated at less than 10%. The DSC/TGA produces results in good agreement with DHA, and can provide HOV as a function of fraction evaporated. A striking feature of the HOV results was the insensitivity of HOV to the hydrocarbon blendstock for temperatures up to 150°C - all four hydrocarbon blendstocks had essentially the same HOV in kJ/kg and exhibited the same HOV response to blending with ethanol. HOV is much less variable than RON or S. HOV at 20% evaporated from the DSC/TGA experiment appeared to be unaffected by ethanol content while HOV at 50% evaporated increased monotonically with ethanol content.

CITATION: Chupka, G., Christensen, E., Fouts, L., Alleman, T. et al., "Heat of Vaporization Measurements for Ethanol Blends Up to 50 Volume Percent in Several Hydrocarbon Blendstocks and Implications for Knock in SI Engines," *SAE Int. J. Fuels Lubr.* 8(2):2015, doi:10.4271/2015-01-0763.

INTRODUCTION AND BACKGROUND

The introduction of more stringent standards for fuel economy as well as greenhouse gas emissions [1] is driving research to increase the efficiency of spark ignition (SI) engines. Approaches for increasing SI engine efficiency include increased compression ratio, direct injection (DI), turbocharging, downsizing, and down-speeding. Higher octane number (more highly knock resistant) fuels allow improved combustion phasing and operation at higher loads at the same engine speed, while also allowing the higher in-cylinder temperature and pressure generated by increased compression ratio and turbocharging which are critical for downsizing and down-speeding [2,3,4]. At the same time, renewable fuel usage is mandated to increase in the United States under the Renewable Fuel Standard [5], and globally under laws enacted in other countries. Ethanol, the most commonly used renewable fuel, has a research octane number (RON) of approximately 110 [6] compared to typical U.S. regular gasoline at 91-93 [2]. Accordingly, high octane number ethanol blends containing from 20 volume percent (vol%) to 40 vol% ethanol are being extensively studied [3, 7,8,9,10]. A unique property of ethanol is its high heat of vaporization (HOV), which significantly increases charge cooling for DI engines, providing additional knock resistance.

The tendency of a spark-ignited engine fuel to autoignite and cause knock is measured as the octane number, a critical performance parameter for SI engines. In the United States, octane number at the retail pump is given as the anti-knock index, the average of two octane number measurements: research octane number (RON) (ASTM D2699-13b) and motor octane number (MON) (ASTM D2700-13b). The primary differences between the RON and MON measurements are fuel-air charge temperature and engine speed, with the RON test using a comparatively low fuel-air charge temperature (that is dependent on the fuel's latent heat of evaporation) and slower engine speed while the MON test is conducted at a significantly higher fuel-air charge temperature (149°C) and faster engine speed. Recent studies have demonstrated that MON is correlated with different effects in modern engines than was the case when these tests were introduced in 1932, and in fact increasing MON at constant RON may actually lower the fuel knock resistance [11]. The

difference between RON and MON is called sensitivity, S = RON - MON, and represents the sensitivity of the fuel autoignition kinetics to the unburned gas temperature [8]. Kalghatgi [12], and Mittal and coworkers [13] have shown that fuels with higher S have slower autoignition kinetics at lower temperatures and faster autoignition kinetics at higher temperatures, compared to fuels with lower S.

Given the high RON of ethanol, it is commonly blended into a sub-octane blendstock for oxygenate blending having RON of approximately 84 to 88 [14] to produce finished gasoline having adequate knock resistance (in terms of the anti-knock index). The RON of blends above E10 has been measured in a variety of research projects [14,15,16,17]. Ethanol has a non-linear effect on the RON of the finished blend, with diminishing effect as the ethanol content is increased. The increase in RON depends on the starting RON of the blendstock, but increases to around 100 to 105 at E50. Ethanol exhibits a MON of 90 (S=20) and imparts sensitivity to hydrocarbon blendstocks with low S.

Fuel knock resistance for DI engines is enhanced by the fact that the fuel-air charge is cooled in the cylinder as the fuel evaporates, reducing the end-gas temperature. This is a major advantage of DI over other SI engine fuel systems and is important regardless of fuel type. However, at 25°C, the HOV of gasoline boiling range hydrocarbons is 350 to 400 kJ/kg while that of ethanol is 924 kJ/kg [3,18]. Because ethanol supplies some oxygen and reduces the amount of air required to burn the fuel, this heat of vaporization advantage is even greater when considered on a per kilogram of stoichiometric mixture basis where the value for hydrocarbon is 22 kJ/kg while that for ethanol is 92 kJ/kg [3]. There is experimental evidence that RON is affected by the HOV of the fuel [19]. However it is not clear that RON captures the full cooling experienced by the intake charge in a DI engine. At E30, this cooling effect may provide the equivalent of 5 to 10 RON units of knock resistance [20].

HOV is also a factor in vehicle driveability. If the fuel requires a higher amount of heat to vaporize at the same temperature, it will not vaporize as readily, in effect, acting like a fuel with a higher T10, T50, or T90 or will be more difficult to vaporize under cold start conditions [21]. The use of an estimation of the amount of heat needed to evaporate sufficient fuel to form an ignitable air-fuel-vapor mixture has been proposed as a fuel property parameter for predicting cold weather driveability [22].

A large database of HOV values for pure compounds has been published [23]. Users of this database are cautioned to carefully examine the source of the data as the database is all inclusive and includes values measured using poorly accurate methods as well as values that upon investigation were not measured, but predicted using various methods. However, the database does contain much high quality data that was measured using many different methods, but which primarily involve either direct or indirect measurement of vapor pressure as a function of temperature. The Clausius-Clapeyron equation is then integrated under the assumption that HOV is constant over a small temperature range and solved for HOV:

$$\ln P = A - HOV/RT \quad (1)$$

where P is pressure, A is a constant of integration, R is the ideal gas constant, and T is temperature. Data for ethanol and several hydrocarbon components of gasoline are shown in Figure 1. HOV decreases as temperature increases attaining a value of zero at the critical temperature. This effect is much larger for ethanol than for the hydrocarbon components. At 25°C, the HOV for ethanol is 924 kJ/kg while that for most hydrocarbon components of gasoline is between 350 to 400 kJ/kg.

Methods for measuring HOV of complex mixtures like gasoline are not well developed. Early studies measured vapor pressure as a function of temperature and applied the Clausius-Clapeyron equation [24, 25]. However, for broad boiling range mixtures like gasoline, the vapor pressure is determined by the most volatile components. For example, several different studies have shown that the initial boiling fractions or container headspace are enriched in the most volatile butane and pentane components of gasoline [26, 27]. This will result in significant errors in the HOV measurement, especially for blends with ethanol given its much higher HOV than gasoline hydrocarbon components.

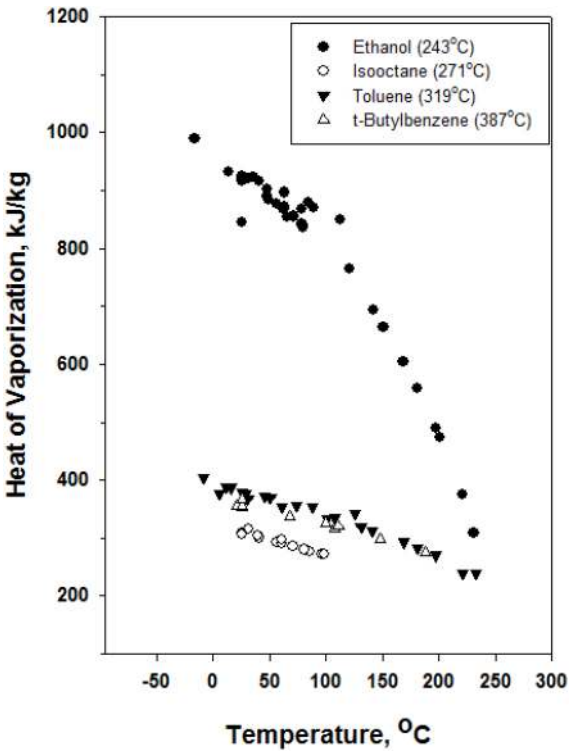

Figure 1. HOV of ethanol and several hydrocarbon components of gasoline, data from Chickos and Acree [23]. Values in parenthesis are the compound's critical temperature where HOV=0.

In principle, differential scanning calorimetry (DSC) could be used to measure gasoline HOV, although we have found no examples of this in the literature [28]. Detailed hydrocarbon analysis (DHA) by gas

chromatography has been used to estimate a number of gasoline properties such as the distillation curve from the pure component boiling points [29] and the octane number from pure component octane numbers [30]. This approach could also be used for estimating HOV. A correlation gas chromatography method has been used to estimate HOV for complex fuel mixtures [31]. This method is an indirect measurement of vapor pressure as a function of temperature for each component of the mixture, and then the Clausius-Clapeyron equation is applied to each component of the mixture.

Our objective has been to develop a clear understanding of how to measure HOV and how to quantify knock resistance for ethanol gasoline blends. Blends of ethanol at nominal 10, 20, 25, 30, 40, and 50 vol% were prepared with three gasoline blendstocks and a natural gasoline (NG). NG is also known as natural gas condensate and is a byproduct of natural gas production consisting primarily of pentanes. Performance properties and composition of the blendstocks were measured. A similar set of properties were measured for the ethanol blends, including RON, MON, net heating value, density, distillation curve, and vapor pressure. HOV was measured by DSC/TGA and estimated from DHA.

METHODS

Fuels

Gasoline blendstocks were obtained from petroleum refiners or local suppliers. These include a wintertime conventional blendstock for oxygenate blending (wCBOB), a California Air Resources Board reformulated blendstock (CARBOB), and a summer class AA blendstock from an ozone non-attainment area (sCBOB). An NG sample was obtained from a mid-stream company. Chemical-grade anhydrous ethanol was used. With the exception of blends in sCBOB, which were prepared volumetrically at room temperature, blending was performed using fuel that had been stored in a freezer overnight prior to blending. Using the densities of the base fuel and of the ethanol, the weight of each component needed to reach the target volume percent was calculated for each blend level and the fuel was blended by weight. Volume percent was measured by gas chromatography using ASTM Method D5501 for all blends. Samples were stored in a freezer in glass or aluminum containers with care to avoid excess headspace.

Fuel Properties

ASTM methods were used as written for most fuel properties. RON and MON tests were conducted at Southwest Research Institute.

DHA was performed by ASTM method D6729. In brief, a gas chromatograph equipped with a flame ionization detector and a cryogenic oven cooling valve was utilized for analysis. A Rtx-100 DHA (Restek, Bellefonte, PA) column of dimensions 100 m × 0.25 mm, 0.5 µm film thickness was used for separation of the hydrocarbons. The helium carrier gas was set to a flow rate of 2 mL/min in constant flow mode. The oven was programmed as follows: 0°C for 15 minutes, followed by a ramp of 1°C/min to 50°C, then 2°C/min to 130°C, then 4°C/min to 270°C with a 5 min hold. The flame ionization detector was set to 300°C, and the flow rates were: 40 mL/min for hydrogen, 450 mL/min for air, and 30mL/min for nitrogen. The injection port was set to 250°C, and samples were injected neat at 0.2 µL with a split ratio of 200:1. In order to identify the individual components, a certified hydrocarbon standard provided by Separation Systems (Gulf Breeze, FL) was used to determine individual hydrocarbon retention times for generation of DHA reports with its Hydrocarbon Expert 5 (HCE5) software. Once the components were identified and quantified, an Excel spreadsheet listing each component and the mole percent (mol%) present was generated. Because there were a few hundred components we eliminated any component that was <0.05 mol% which resulted in less than a 5% total reduction in sample.

HOVs of individual compounds were predicted at given temperatures following the method proposed by Reid, Prausnitz, and Poling [32]:

$$\frac{HOV}{RT_c} = 7.08(1-T_r)^{0.354} + 10.95\omega(1-T_r)^{0.456} \quad (2)$$

where HOV is the heat of vaporization, R is the gas constant (0.008314 kJ/mol K), T_c is the critical temperature, T is the desired temperature, T_r is the reduced temperature (T/T_c), and ω is the acentric factor. Critical temperature and acentric factor for individual compounds were taken from literature sources [33, 34].

The predicted HOVs in kJ/mol were multiplied by the mol% of each component present and then totaled. This value was divided by the total mol% of the sample (after removal of the minor components) and then divided by the average molecular weight of the gasoline (this value is also calculated by the HCE5 software) to give the HOV in kJ/kg. For ethanol blends the ethanol content measured by ASTM method D5501 and the predicted HOV of ethanol at the given temperature were factored into this calculation.

HOV was measured using a DSC/TGA method. A DSC/TGA Q600 (TA Instruments, Newcastle, DE) was used for all experiments. The instrument was calibrated using sapphire as a standard for heat flow and alumel and nickel as standards for weight loss. The instrument's cell constant was further calibrated using deionized water. Water was run three times and the HOVs were calculated and averaged. The average was compared to the reported literature value for water and the literature value/measured value ratio was calculated. All subsequent sample measurements were adjusted by this value.

Samples were prepared by storing them in a container with dry ice to limit evaporation during transfer to the sample pan. The sample was injected via microliter syringe into a 50 microliter aluminum pan (Mettler Toledo part# ME-51119872) with 75 µm laser drilled pin-hole aluminum lids (TA Instruments part# 900860.901) and a sample transfer time of 30 seconds. The experiment was initiated immediately upon loading of the sample into the instrument at a constant temperature of 23°C and nitrogen flow of 100 mL/min.

The heat flow values were corrected for zero heat flow by subtracting the baseline value measured after the sample had evaporated from the measured heat flow at each point. Heat flow at each point in time was then corrected for the cell constant determined from calibration of the

instrument with deionized water. The DSC data were plotted as heat flow (in milliwatts) versus time (see example in Figure 2), and the area under the curve was estimated using the trapezoid method. This corrected area under the curve is the total heat flow to the sample in millijoules required for evaporation. This value was divided by the total mass of the sample to give the sample total HOV. The HOV of pure ethanol was measured as 936 kJ/kg which is within 1.3% of the 924 kJ/kg value commonly reported in the literature [3, 18]. The heat flow and TGA (sample mass) data were combined to estimate a HOV as a function of mass fraction of sample evaporated.

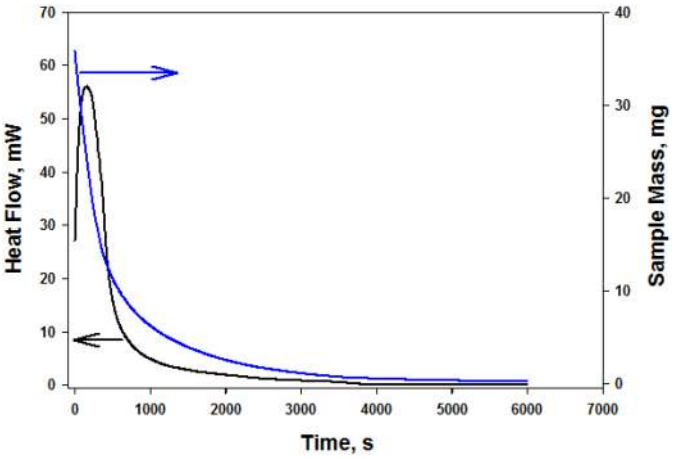

Figure 2. Heat flow (baseline corrected) and mass loss curves from the DSC/ TGA experiment for 30 vol% ethanol in CARBOB.

RESULTS AND DISCUSSION

Fuel Properties

Paraffin, isoparaffin, aromatic, naphthene, and olefin (PIANO) analyses from the detailed hydrocarbon analysis of the hydrocarbon blendstocks are reported in Table 1. The wCBOB and sCBOB have about 25 vol% aromatics - in the range typical for gasoline in North America, while the CARBOB would be considered low aromatic content gasoline [35]. The NG is almost entirely paraffinic. Table A-1,A-2,A-3,A-4 in the Appendix present the properties of the hydrocarbon blendstocks as well as their ethanol blends. Our intent was to have blendstocks covering a broad range of properties, especially volatility, available in the market today. The blendstocks have vapor pressure as dry vapor pressure equivalent (DVPE) ranging from 6.1 psi (42 kPa) to 13.8 psi (95 kPa) and T90 ranging from 100°C to 172°C. Note that actual ethanol content differed somewhat from nominal (or target) values, especially for the 40% and 50% blends.

Figure 3 shows RON as a function of ethanol content. While the blendstocks have RON values that differ by up to 23 RON units, above 30% to 40% ethanol the curves converge at a RON of 103 to 105, even for the much lower RON NG sample. Figure 4 shows octane sensitivity (S) which increases significantly as ethanol is blended into the various blendstocks. Unlike RON, which appears to converge at a single or narrow range of values for high ethanol content, there are significant differences in S at high ethanol levels. Gasoline blendstocks with nearly identical S can show significantly different sensitivities when blended with ethanol.

Table 1. PIANO analysis (ASTM D6729) and volatility properties for the hydrocarbon gasoline blendstocks.

Group	wCBOB	CARBOB	sCBOB	NG
Paraffin, vol%	9.59	7.65	11.5	37.7
I-Paraffins, vol%	56.1	53.6	47.9	42.9
Aromatics, vol%	25.8	15.6	23.7	3.72
Naphthenes, vol%	4.71	13.0	7.8	14.8
Olefins, vol%	3.60	8.09	8.4	0.712
Average Molecular Weight (DHA)	96.3	100.5	95.9	80.2
C, wt% (DHA)	85.9	85.6	86.1	84.1
H, wt% (DHA)	14.1	14.4	13.9	15.9
DVPE, kPa (ASTM D5191)	76	42	46	95
T_{10}, °C (ASTM D86)	43	65	61	39
T_{50}, °C (ASTM D86)	101	106	98	52
T_{90}, °C (ASTM D86)	172	156	154	100

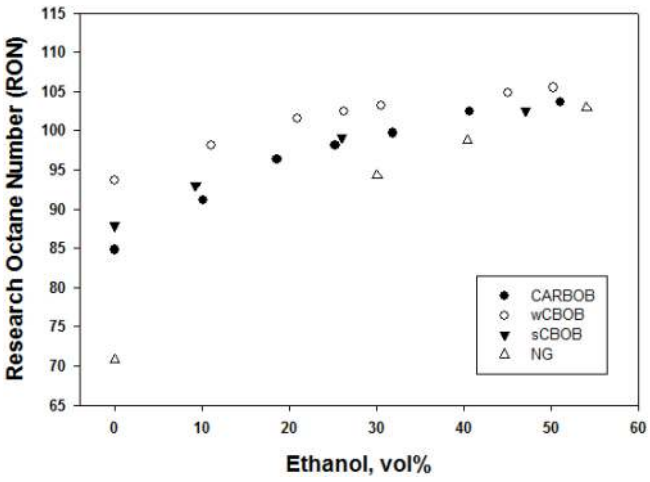

Figure 3. RON measured for ethanol-gasoline blends.

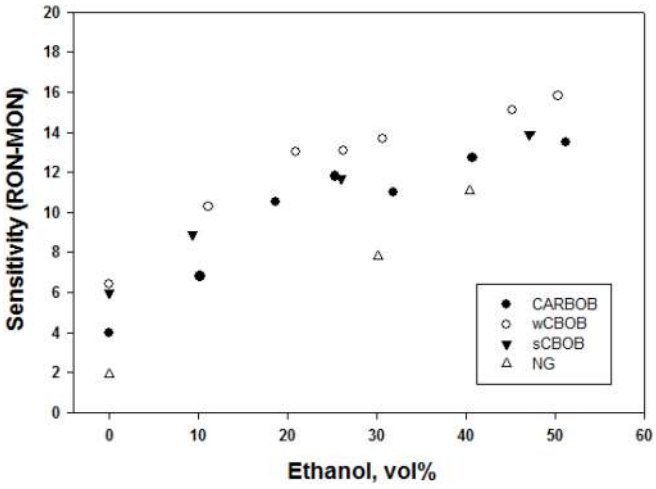

Figure 4. Octane sensitivity for ethanol-gasoline blends.

Heat of Vaporization

HOV by Detailed Hydrocarbon Analysis

Figure 5 shows HOV as a function of temperature for the four hydrocarbon blendstocks. Up to 100°C, all four blendstocks show nearly identical results, with HOV declining from 350 kJ/kg at 25°C to 300 kJ/kg at 100°C, in spite of the broad range of volatility. At higher temperatures, the NG sample begins to exhibit a lower HOV than the other blendstocks, likely because it consists primarily of butanes and pentanes, which have a much lower critical temperature than the average for the three other blendstocks.

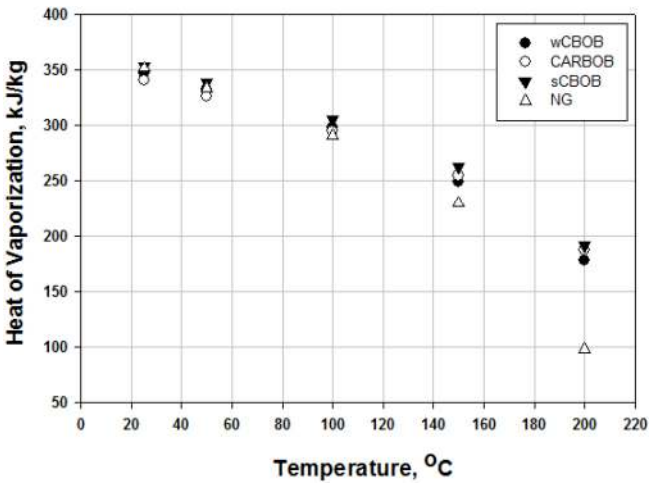

Figure 5. HOV as a function of temperature estimated from DHA for the four hydrocarbon blendstocks.

HOV as a function of temperature and ethanol content for the ethanol-hydrocarbon blends is shown in Figure 6 for all four blendstocks. At 25°C there is a linear increase in HOV from 350 kJ/kg to approximately 700 kJ/kg at nominally E50. The trends are essentially identical for all blendstocks up to 150°C, that is, blends of ethanol in all four hydrocarbons exhibit nearly the same HOV at a given ethanol content and temperature. At 200°C, the NG and its blends fall well below the trend line consistent with the blendstock composition and their lower critical temperatures. This effect becomes less pronounced with increasing ethanol content as the 50 vol% blend is over 70 mol% ethanol. Individual plots of HOV as a function of temperature and ethanol content for each blendstock are shown in Figures A-1,A-2,A-3,A-4 in the Appendix.

Errors in the DHA estimate of HOV can arise from errors in quantification by gas chromatography, elimination of components present at <0.05 mol% representing no more than 5 mol% of the sample in total, and errors in predicting the pure component HOV from equation (2). Based on the published reproducibility of ASTM method D6729 for individual compounds the uncertainty in the total HOV estimate for hydrocarbon blendstocks is 1%. For ethanol blends, this uncertainty is higher due to the lower precision of ethanol concentration by D5501. The uncertainty in HOV of blends is estimated to be below 10% when accounting for uncertainty in hydrocarbon and ethanol measurements. Elimination of the low-concentration components introduces at most a 5% error. Figure 7 reproduces the data shown in Figure 1, and includes predicted values from equation 2. Predictions of HOV for ethanol, isooctane, and toluene are in good agreement with the data while predictions for t-butylbenzene fall significantly below measured values at low temperatures (likely because the correlation is reported to be more accurate for $T_r > 0.6$). While this figure shows results for only a few selected compounds, it is likely that accuracy of the DHA HOV determination could be improved by ensuring that accurate pure component HOV predictions are used.

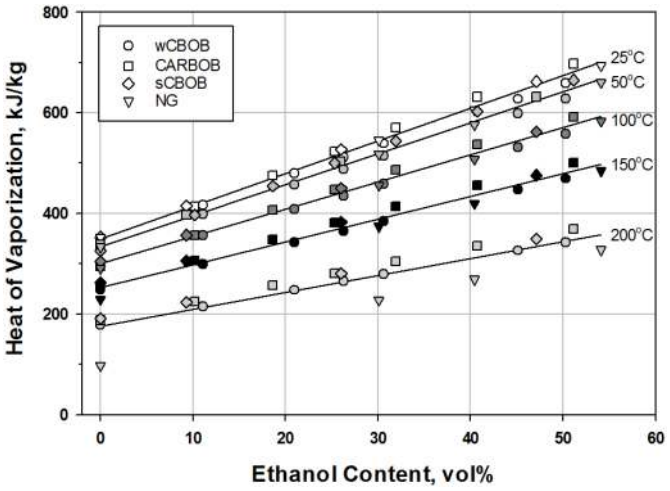

Figure 6. HOV as a function of ethanol content (x-axis) and temperature (symbol color) estimated from DHA for the four hydrocarbon blendstocks.

It is worth noting that the Chen and Stone have measured the heat of mixing for ethanol blends up to 85 vol% in isooctane to be less than 10 kJ/kg [18]. The HOV determination by DHA does not take heat of mixing into account; however this could only introduce a small error.

HOV by DSC/TGA

Figure 8 shows HOV by DSC/TGA as a function of ethanol content at 23°C for wCBOB and CARBOB blends, as well as HOV by DHA at 25°C, for all blends. Initial attempts to measure HOV by DSC/TGA were biased to lower values relative to DHA by about 17% because of sample loss by evaporation during transfer from the dry ice cooler to the instrument. Sample losses ranged from 20% to 25% of the mass of the sample. Injection of the sample via microliter syringe into a 50 microliter closed cup with a laser drilled pin hole reduced sample loss to less than 4% (Table A-5) and also reduced sample transfer time to 30 seconds. With this improved technique results are very consistent with the DHA results (Figure 8). Three repeat HOV measurements by DSC/TGA were performed for the CARBOB E0 and E30 yielding a coefficient of variation of 2.8% and 3.4%, respectively - so the measurement is reasonably precise. As an aside, Figure 8 also shows results presented for HOV of ethanol gasoline blends in reference 25, obtained by measuring vapor pressure as a function of temperature and applying the Clausius-Clapeyron equation. On average these values fall significantly below those derived from DHA or measured by DSC/TGA, especially at higher ethanol levels.

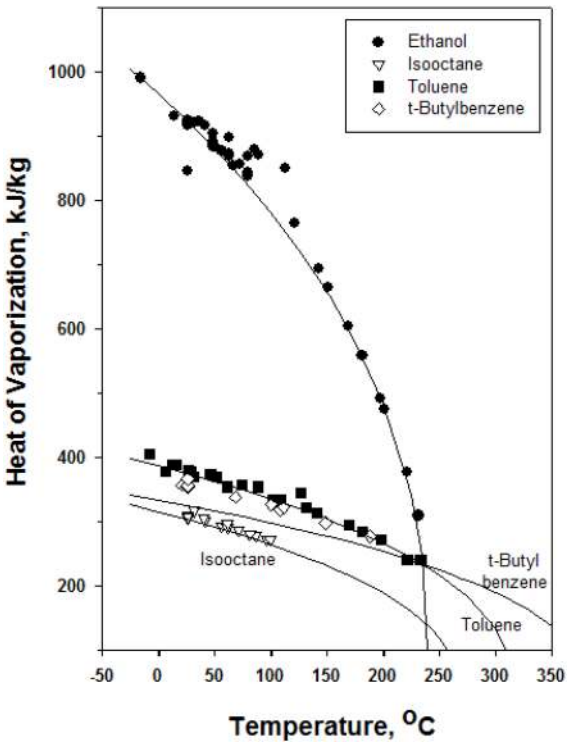

Figure 7. Comparison of HOV measured for pure components with predicted values from equation (2) (solid lines). Data from Chickos and Acree [23].

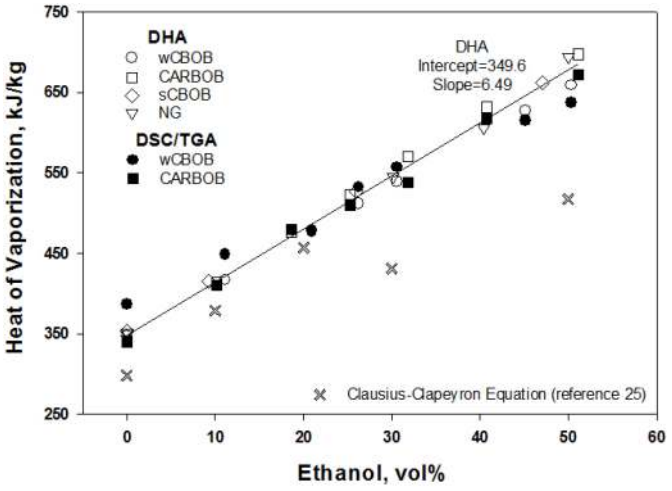

Figure 8. HOV as a function of ethanol content measured by DSC/TGA (CARBOB blends) at 23°C and by DHA (all blends) at 25°C.

The DSC/TGA approach has the advantage of providing a measurement of HOV as a function of fraction evaporated. These data are shown in Figures 9 for the CARBOB blends (results for wCBOB are similar, see Figure A-5). Distillation curves for ethanol-gasoline blends show a flattening around T50 as the ethanol-gasoline mixture exhibits azeotrope-like behavior, especially at higher blend levels (see results for CARBOB and blends in Figure A-6). The DSC/TGA curves do not show this flattening because the cumulative HOV increases monotonically as fuel evaporates. The heat required to evaporate the first (approximately) 20 wt% of the gasoline is an important parameter for engine cold start [21]. Figure 10 shows there is at most a small effect of ethanol content on HOV 0.2 (HOV at 20% evaporated) although the precision of the data does not appear to be adequate to make a quantitative estimate of this effect. The heat required to evaporate 50% of the gasoline can affect hot weather driveability [21]. HOV 0.5 increases with ethanol content, with a near doubling of the heat effect for E50. Overall there do not appear to be significant differences in the results for the winter and summer gasoline blendstocks. Additional research is required to improve the precision of HOV as a function of fraction evaporated measurements.

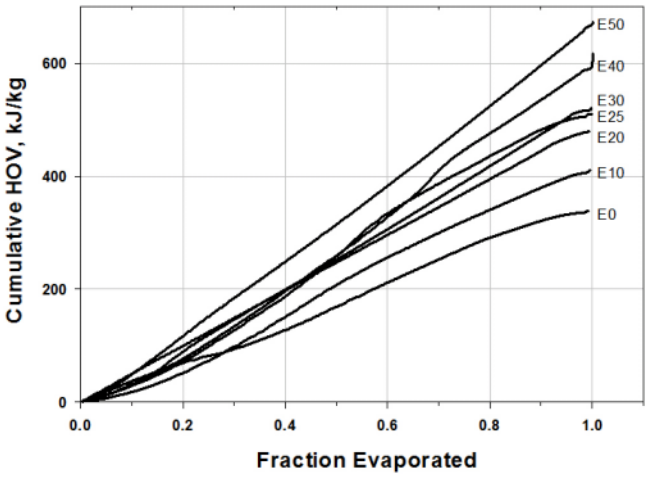

Figure 9. HOV by DSC/TGA as a function of fraction evaporated for ethanol blends in CARBOB at 23°C.

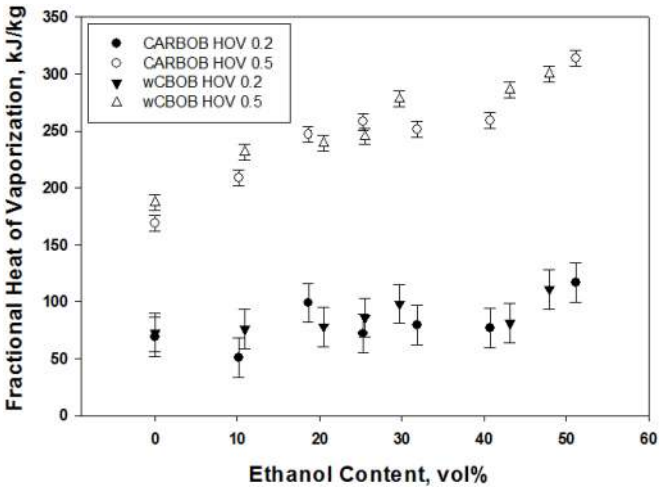

Figure 10. HOV at 20% and 50% evaporated by DSC/TGA as a function of fraction evaporated at 23°C. Error bars are 95% confidence interval based on three replications on E30.

Adiabatic Cooling of Stoichiometric Air-Fuel Mixture

The temperature drop for evaporation of the fuel into a stoichiometric mass of air is a useful theoretical metric for charge cooling in a DI engine. For ethanol blends this calculated value encompasses both the increased HOV of the fuel and the significantly lower stoichiometric air-to-fuel mass ratio that is a consequence of oxygenate blending (air-to-fuel mass ratio drops from roughly 14.6 at E0 to 11.7 at E50). This is the theoretical maximum possible cooling and Kasseris and Heywood suggest that actual cooling in a DI engine for blends up to 50 vol% ethanol will be about 70% of the theoretical maximum value [20].

The temperature drop for adiabatic evaporation of the blends in a stoichiometric quantity of air was calculated at 25°C, 50°C, 100°C and 150°C (initial air and fuel temperature) using the HOV derived from DHA and equation (3):

$$\Delta T_{ad} = m_{fuel}\, HOV/(m_{fuel} + m_{air})C_{p\text{-}mixture} \quad (3)$$

where ΔT_{ad} is the temperature change for adiabatic cooling, m_{fuel} isthe mass of fuel, HOV is the heat of vaporization, m_{air} is the mass of air, and $C_{p\text{-}mixture}$ is the heat capacity at constant pressure of the fuel-air mixture. An average heat capacity of the mixture at the initial temperature was calculated on a weight basis with values obtained from the literature [36, 37]. Figure 11 shows the theoretical temperature change for evaporation of ethanol blends. The cooling estimated at every ethanol level is in reasonable agreement with that calculated by Kasseris and Heywood [38]. There is only a small reduction in cooling for increasing initial temperature from 25°C to 50°C, but increasing to 100°C will result in a significant loss of evaporative charge cooling at high ethanol blend levels. Because all hydrocarbon blendstocks examined have about the same HOV, and the same HOV response to ethanol blending, adiabatic charge cooling is a function of temperature and ethanol content only, to a good approximation.

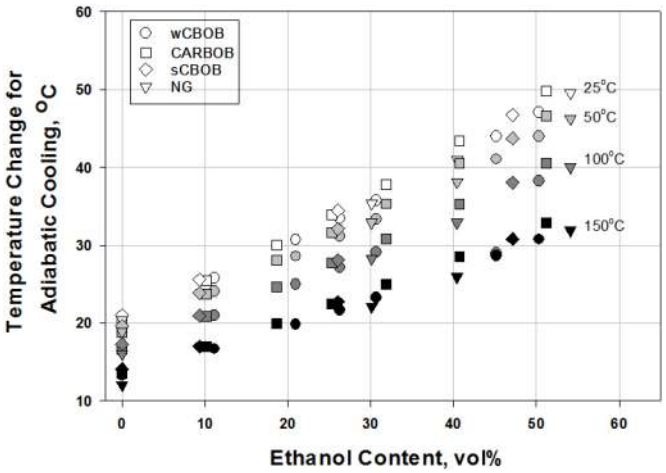

Figure 11. Temperature change for adiabatic cooling of stoichiometric air-fuel mixtures, initial temperature listed at right.

SUMMARY/CONCLUSIONS

The objective of this work was to measure knock resistance metrics for ethanol-hydrocarbon blends with a primary focus on development of methods to measure the HOV. Blends of ethanol at 10 to 50 vol% were prepared with three gasoline blendstocks and an NG. Performance properties and composition of the blendstocks and blends were measured, including RON, MON, net heating value, density, distillation curve, and vapor pressure. HOV was estimated from DHA as well as using a DSC/TGA method.

RON increases upon blending ethanol but with diminishing returns above about 30 vol%. Above 30% to 40% ethanol the curves flatten and converge at a RON of about 103 to 105, even for the much lower RON NG blendstock. Octane sensitivity (S = RON - MON) also increases upon ethanol blending. Gasoline blendstocks with nearly identical S can show significantly different sensitivities when blended with ethanol.

The DHA method allows relatively straight forward estimation of fuel composition and temperature effects with errors estimated at less than 15%. Given that care is taken to avoid sample loss to prior to starting the experiment, the DSC/TGA method gives results in good agreement with DHA, and can also provide HOV as a function of fraction evaporated. A striking feature of the results was the insensitivity of HOV to hydrocarbon blendstock for temperatures up to 150°C - all four hydrocarbon blendstocks tested had essentially the same HOV in kJ/kg and responded the same for blending of ethanol. Because of this, the theoretical temperature change for evaporation of the fuel into a stoichiometric mass of air is to a good approximation a function of initial air temperature and ethanol content only, independent of hydrocarbon blendstock. If additional research shows that this result is general for all gasoline blendstocks, then both HOV and adiabatic stoichiometric mixture cooling could easily and accurately be estimated from an empirical correlation. These parameters are much less variable than gasoline blendstock or ethanol blend RON and S. Relevant to vehicle cold start and driveability, HOV at 20% evaporated from the DSC/TGA experiment appeared to be unaffected by ethanol content while HOV at 50% evaporated increased monotonically with ethanol content.

ACKNOWLEDGMENTS

This work was supported by the U.S. Department of Energy, Bioenergy Technologies Office, under Contract No. DE347AC36-99GO10337 with the National Renewable Energy Laboratory.

CONTACT INFORMATION

Robert McCormick
robert.mccormick@nrel.gov

REFERENCES

1. U.S. Environmental Protection Agency, “EPA and NHTSA Set Standards to Reduce Greenhouse Gases and Improve Fuel Economy for Model Years 2017-2025 Cars and Light Trucks” EPA-420-F-12-051, August 2012.
2. Anderson, J.E., DiCicco, D.M., Ginder, J.M., Kramer, U., Leone, T.G., Raney-Pablo, H.E., and Wallington, T.J., “High Octane Number Ethanol-Gasoline Blends: Quantifying the Potential Benefits in the United States,” *Fuel* 97: 585-594, 2012.
3. Stein, R., Anderson, J., and Wallington, T., “An Overview of the Effects of Ethanol-Gasoline Blends on SI Engine Performance, Fuel Efficiency, and Emissions,” *SAE Int. J. Engines* 6(1):470-487, 2013, doi:10.4271/2013-01-1635.
4. Chow, E., Heywood, J., and Speth, R., “Benefits of a Higher Octane Standard Gasoline for the U.S. Light-Duty Vehicle Fleet,” SAE Technical Paper 2014-01-1961, 2014, doi:10.4271/2014-01-1961.
5. Energy Independence and Security Act of 2007, Public Law110-140, Title II, Subtitle A, Sec. 202. Renewable Fuel Standard, December 19, 2007.
6. Christensen, E., Yanowitz, J., Ratcliff, M., and McCormick, R.L., “Renewable Oxygenate Blending Effects on Gasoline Properties” *Energy Fuels* 25: 4723-4733, 2011.
7. Milpied, J., Jeuland, N., Plassat, G., Guichaous, S. et al., “Impact of Fuel Properties on the Performances and Knock Behaviour of a Downsized Turbocharged DI SI Engine - Focus on Octane Numbers and Latent Heat of Vaporization,” *SAE Int. J. Fuels Lubr.* 2(1):118-126, 2009, doi:10.4271/2009-01-0324.

8. Stein, R., Polovina, D., Roth, K., Foster, M. et al., "Effect of Heat of Vaporization, Chemical Octane, and Sensitivity on Knock Limit for Ethanol - Gasoline Blends," *SAE Int. J. Fuels Lubr.* 5(2):823-843, 2012, doi:10.4271/2012-01-1277.
9. Splitter, D.A., and Szybist, J.P., "Experimental Investigation of Spark-Ignited Combustion with High-Octane Biofuels and EGR.1.Engine Load Range and Downsize Downspeed Opportunity," *Energy Fuels* 28(2):1418-1431, 2014.
10. Leone, T., Olin, E., Anderson, J., Jung, H. et al., "Effects of Fuel Octane Rating and Ethanol Content on Knock, Fuel Economy, and CO2 for a Turbocharged DI Engine," *SAE Int. J. Fuels Lubr.* 7(1):9-28, 2014, doi:10.4271/2014-01-1228.
11. Mittal, V. and Heywood, J., "The Shift in Relevance of Fuel RON and MON to Knock Onset in Modern SI Engines Over the Last 70 Years," *SAE Int. J. Engines* 2(2):1-10, 2010, doi:10.4271/2009-01-2622.
12. Kalghatgi, G., "Fuel Anti-Knock Quality- Part II. Vehicle Studies - How Relevant is Motor Octane Number (MON) in Modern Engines?," SAE Technical Paper 2001-01-3585, 2001, doi:10.4271/2001-01-3585.
13. Mittal, V., Heywood, J., and Green, W., "The Underlying Physics and Chemistry behind Fuel Sensitivity," *SAE Int. J. Fuels Lubr.* 3(1):256-265, 2010, doi:10.4271/2010-01-0617.
14. American Petroleum Institute, "Determination of the Potential Property Ranges of Mid-Level Ethanol Blends, Final Report," April 23, 2010.
15. Anderson, J., Leone, T., Shelby, M., Wallington, T. et al., "Octane Numbers of Ethanol-Gasoline Blends: Measurements and Novel Estimation Method from Molar Composition," SAE Technical Paper 2012-01-1274, 2012, doi:10.4271/2012-01-1274.
16. Bielaczyc, P., Woodburn, J., Klimkiewicz, D., Pajdowski, P., and Szczotka, A., "An Examination of the Effect of Ethanol-Gasoline Blends' Physicochemical Properties on Emissionsfrom a Light-Duty Spark Ignition Engine," *Fuel Processing Technology* 107: 50-63, 2013.
17. Yanowitz, J., Knoll, K., Kemper, J., Luecke, J., and McCormick, R.L., "Impact of Adaptation of Flex-Fuel Vehicle Emissions When Fueled with E40," *Environ. Sci. Technol.* 47: 2990-2997,2013.
18. Chen, L., and Stone, R., "Measurement of Enthalpies of Vaporization of Isooctane and Ethanol blends and Their Effectson PM Emissions from a GDI Engine," *Energy Fuels* 25:1254-1259, 2011.
19. Foong, T., Morganti, K., Brear, M., da Silva, G. et al., "The Effect of Charge Cooling on the RON of Ethanol/Gasoline Blends," *SAE Int. J. Fuels Lubr.* 6(1):34-43, 2013, doi:10.4271/2013-01-0886.
20. Kasseris, E. and Heywood, J., "Charge Cooling Effects on Knock Limits in SI DI Engines Using Gasoline/Ethanol Blends: Part 2-Effective Octane Numbers," *SAE Int. J. Fuels Lubr.* 5(2):844-854, 2012, doi:10.4271/2012-01-1284.
21. Stradling, R., Antunez Martel, F-J., Ariztegui, J., Beeckmann, J., et al. "Volatility and Vehicle Driveability Performance of Ethanol/Gasoline Blends: A Literature Review," CONCAWE Report No. 8/09, October 2009, www.concawe.org.
22. Harrison, A., "Enthalpy Requirement-A New Fundamentally-Based Gasoline Volatility Parameter For Predicting Cold-Weather Driveability," SAE Technical Paper 881670, 1988, doi:10.4271/881670.
23. Chickos, J.S., and Acree, W.E., "Enthalpies of Vaporization of Organic and Organometallic Compounds, 1880-2002," *J. Phys. Chem. Ref. Data* 32:519-878, 2003.
24. Balabin, R.M., Syunyaev, R.Z., and Karpov, S.A., "Molar Enthalpy of Vaporization of Ethanol-Gasoline Mixtures and Their Colloidal State," *Fuel* 86: 323-327, 2007.
25. Kar, K., Last, T., Haywood, C., and Raine, R., "Measurement of Vapor Pressures and Enthalpies of Vaporization of Gasoline and Ethanol Blends and Their Effects on Mixture Preparation in an SI Engine," *SAE Int. J. Fuels Lubr.* 1(1):132-144, 2009, doi:10.4271/2008-01-0317.
26. Harley, R.A., Coulter-Burke, S.C., and Yeung, T.S., "Relating Liquid Fuel and Headspace Vapor Composition for California Reformulated Gasoline Samples Containing Ethanol," *Environ. Sci. Technol.* 34:4088-4094, 2000.
27. Smith B.L., and Bruno, T.J., "Improvements in the Measurement of Distillation Curves. 3. Application to Gasoline and Gasoline + Methanol Mixtures," *Ind. Eng. Chem. Res.* 46:297-309, 2007.
28. Mita, I., Imai, I., and Kambe, H., "Determination of Heat of Mixing and Heat of Vaporization with A Differential Scanning Calorimeter," *Thermochimica Acta* 2:337-344, 1971.
29. ASTM International, "Standard Test Method for Calculated Flash Point from Simulated Distillation Analysis of Distillate Fuels," ASTM Standard D7215-08(2013), 2013. www.astm.org
30. Ghosh, P., Hickey, K.J., and Jaffe, S.B., "Development of a Detailed Gasoline Composition-Based Octane Model," *Ind. Eng. Chem. Res.* 45:337-345, 2006.
31. Chickos, J. S., Hosseini, S., and Hesse, D.G., "Determination of Vaporization Enthalpies of Simple Organic Molecules by Correlations of Changes in Gas Chromatographic Net Retention Times," *Thermochimica Acta* 249:41-62, 1995.
32. Reid, R.C., Prausnitz, J.M., and Poling, B.E., "The Properties of Gases and Liquids," 4th ed., (New York, McGraw-Hill, 1987).
33. API Technical Data Book - Petroleum Refining, API, 1993.
34. Yaws, C.L. Yaws' Handbook of Thermodynamic and Physical Properties of Chemical Compounds: Physical, Thermodynamic and Transport Properties for 5,000 Organic Chemical Compounds. McGraw-Hill, 2003.
35. AAM Alliance of Automobile Manufacturers North American Fuel Survey, 2011.
36. National Institute of Standards and Technology, "Ethanol," http://webbook.nist.gov/cgi/cbook.cgi?ID=C64175&Mask=2, accessed May 29, 2014.
37. The Engineering Toolbox, "Liquids and Fluids - Specific Heats." http://www.engineeringtoolbox.com/specific-heat-fluids-d_151.html, accessed May 29, 2014.
38. Kasseris, E. and Heywood, J., "Charge Cooling Effects on Knock Limits in SI DI Engines Using Gasoline/Ethanol Blends: Part 1-Quantifying Charge Cooling," SAE Technical Paper 2012-01-1275, 2012, doi:10.4271/2012-01-1275.

DEFINITIONS/ABBREVIATIONS

CARBOB - California Air Resources Board reformulated blendstock for oxygenate blending

CBOB - Conventional blendstock for oxygenate blending

DHA - Detailed hydrocarbon analysis

DI - Direct injection

DSC - Differential scanning calorimetry

DVPE - Dry vapor pressure equivalent (modern equivalent of RVP)

HOV - Heat of vaporization

mol% - Mole percent

MON - Motor octane number

NG - Natural gasoline

PIANO - Paraffin, isoparaffins, aromatic, naphthene, and olefin

RON - Research octane number

RVP - Reid vapor pressure

S - Octane sensitivity (RON-MON)

sCBOB - Summer class AA blendstock from an ozone non-attainment area

SI - Spark ignition

TGA - Thermogravimetric analysis

vol% - Volume percent

wCBOB - wintertime conventional blendstock for oxygenate blending

ΔT_{ad} - Temperature decrease for adiabatic cooling of a stoichiometric fuel air mixture

APPENDIX

Table A-1. Properties of wCBOB and ethanol blends.

Nominal EtOH		vol%	0	10	20	25	30	40	50
Actual EtOH	D5501	vol%	--	11.11	20.94	26.25	30.63	45.15	50.32
Density at 15°C	D4052	g/ml	0.7242	0.7462	0.7494	0.7534	0.7549	0.7658	0.7685
DVPE (RVP eq)	D5191	psi	10.99	11.85	11.46	11.22	11.02	10.20	9.75
Net Heating Value	D240	MJ/L	31.55	30.92	29.51	28.88	28.56	26.69	26.50
HOV (DHA)	NREL	kJ/kg	346.7	417.0	478.9	511.7	539.1	627.3	658.8
RON	D2699		93.7	98.1	101.6	102.5	103.2	104.8	105.5
MON	D2700		87.3	87.8	88.6	89.4	89.5	89.7	89.7
Stoichiometric Air-Fuel Ratio			14.689	14.001	13.405	13.087	12.827	11.982	11.686

Table A-2. Properties of CARBOB and ethanol blends.

Nominal EtOH		Vol%	0	10	20	25	30	40	50
Actual EtOH	D5501	vol%	--	10.16	18.64	25.31	31.88	40.71	51.14
Density at 15°C	D4052	g/ml	0.7318	0.7357	0.7416	0.7446	0.7477	0.7544	0.7602
DVPE (RVP eq)	D5191	psi	6.12	7.09	6.94	6.91	6.83	6.69	6.50
Net Heating Value	D240	MJ/L	32.01	30.89	29.75	29.07	28.56	27.59	26.35
HOV (DHA)	NREL	kJ/kg	340.3	414.4	475.5	523.4	570.2	631.6	697.4
RON	D2699		84.8	91.1	96.4	98.1	99.7	102.4	103.6
MON	D2700		80.8	84.3	85.9	86.3	88.7	89.7	90.1
Stoichiometric Air-Fuel Ratio			14.757	14.126	13.607	13.204	12.812	12.291	11.686

Table A-3. Properties of sCBOB and ethanol blends.

Nominal EtOH		Vol%	0	10	25	50
Actual EtOH	D5501	vol%	--	9.3	26.0	47.1
Density at 15°C	D4052	g/ml	0.7374	0.7432	0.7497	0.7625
DVPE (RVP eq)	D5191	psi	6.73	7.24	7.23	6.71
Net Heating Value	D240	MJ/L	32.1	30.8	29.1	26.8
HOV (DHA)	NREL	kJ/kg	352.8	415.5	527.2	662.2
RON	D2699		87.9	93.0	99.1	102.6
MON	D2700		81.9	84.1	87.4	88.7
Stoichiometric Air-Fuel Ratio			14.643	14.085	13.099	11.884

Table A-4. Properties of NG and ethanol blends.

Nominal EtOH		Vol%	0	30	40	50
Actual EtOH	D5501	vol%	--	30.1	40.4	54.1
Density at 0°C	D4052	g/ml	0.6700	0.7050	0.7182	0.7323
DVPE (RVP eq)	D5191	psi	13.82	13.61	12.99	12.41
Net Heating Value	D240	MJ/L	29.9	27.1	25.9	23.2
HOV (DHA)	NREL	kJ/kg	351.6	545.2	605.9	693.6
RON	D2699		70.8	94.3	98.8	102.9
MON	D2700		68.9	86.5	87.7	--
Stoichiometric Air-Fuel Ratio			15.098	13.150	12.506	11.666

Table A-5. Mass loss by evaporation over one minute in laser pin hole drilled closed cup DSC sample pans.

Time, s	E30 Run 1	E30 Run2	E30 Run 3
0	35.37	37.3	35.68
10	35.1	36.98	35.28
20	34.75	36.41	34.75
30	34.31	35.78	34.25
mg loss/min	1.06	1.52	1.43
% Loss	3.00	4.08	4.01
Average, %			3.69

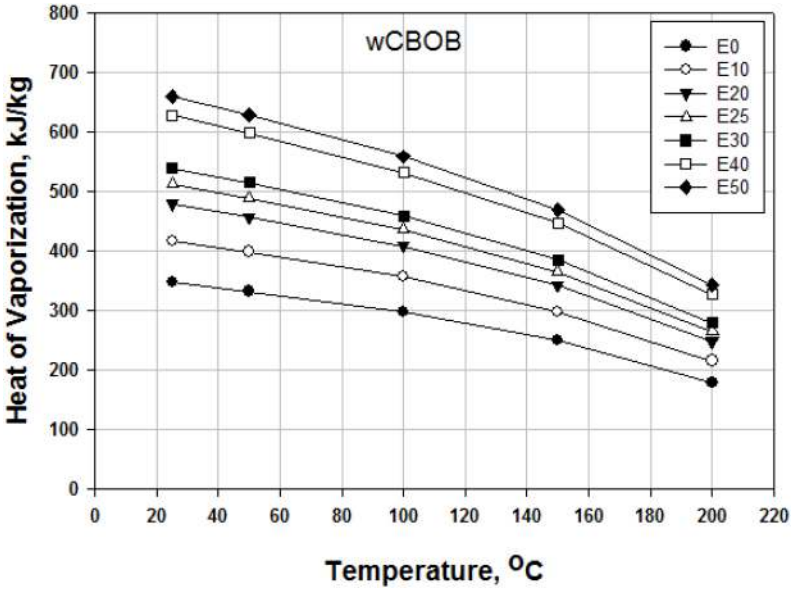

Figure A-1. HOV estimated by DHA as a function of temperature and ethanol content for wCBOB blends.

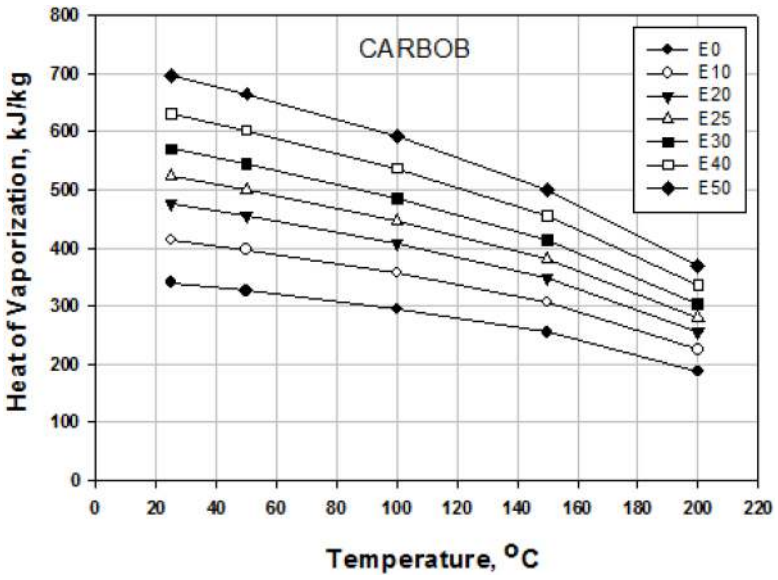

Figure A-2. HOV estimated by DHA as a function of temperature and ethanol content for CARBOB blends.

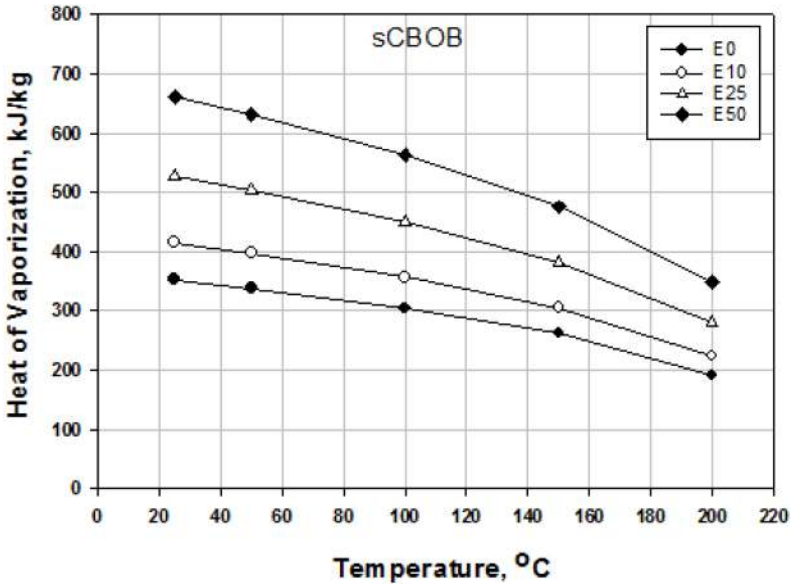

Figure A-3. HOV estimated by DHA as a function of temperature and ethanol content for sCBOB blends

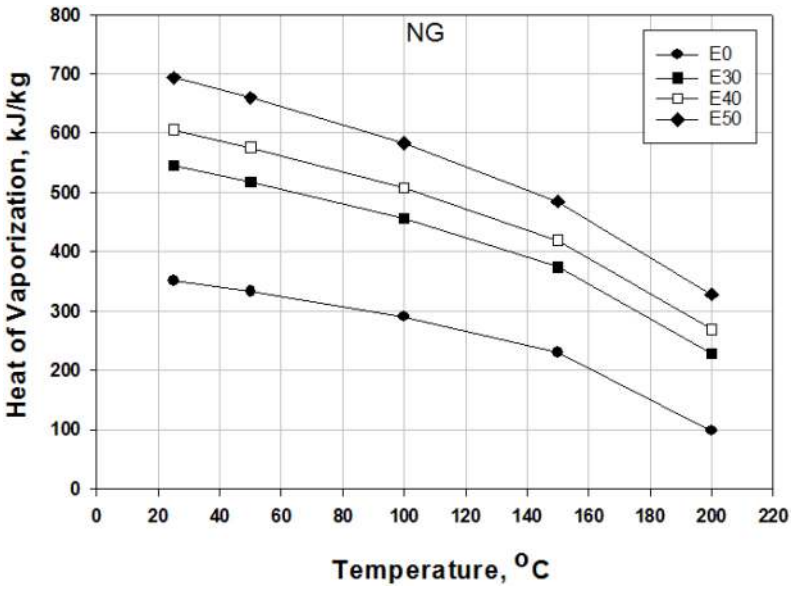

Figure A-4. HOV estimated by DHA as a function of temperature and ethanol content for NG blends.

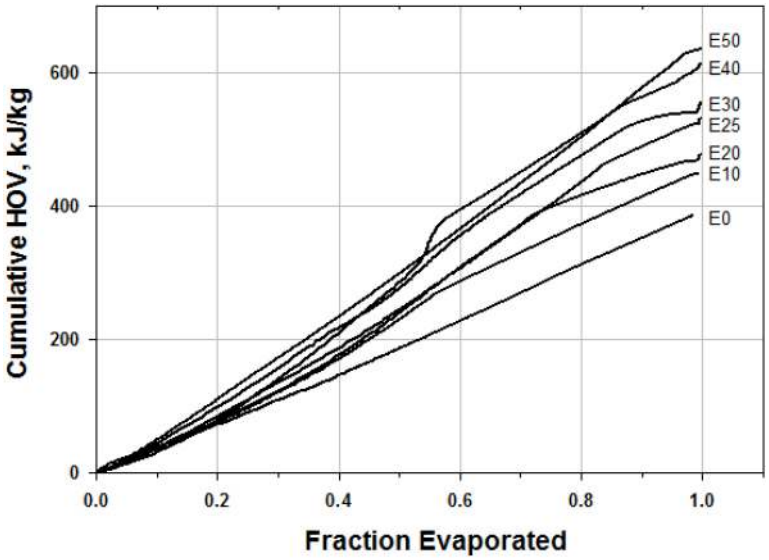

Figure A-5. HOV by DSC/TGA as a function of fraction evaporated for ethanol blends in wCBOB at 23°C.

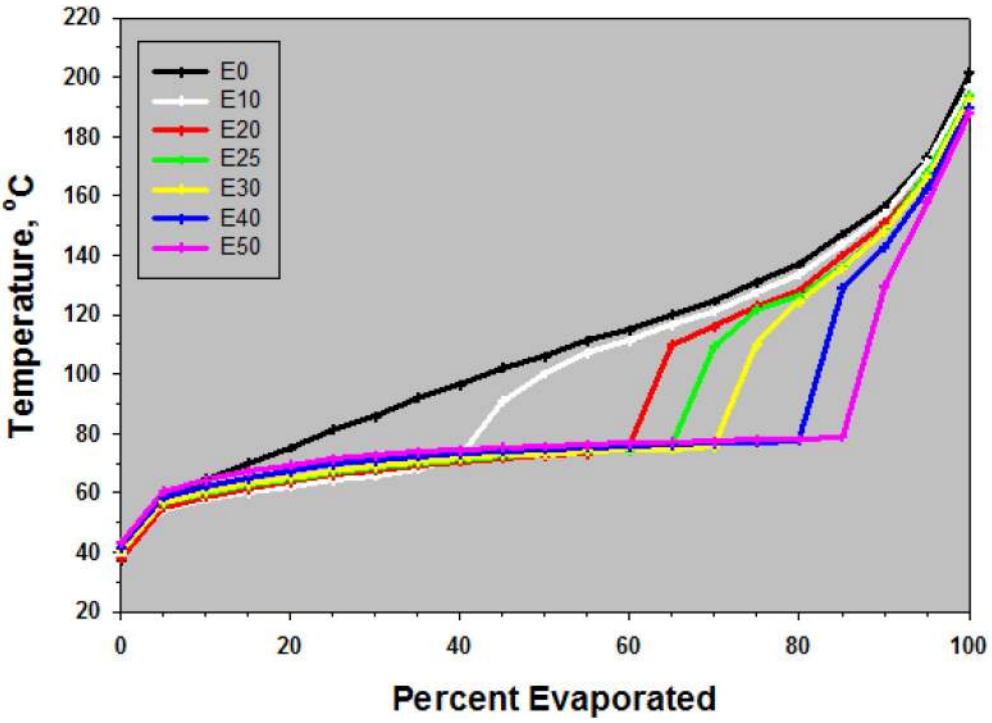

Figure A-6. Distillation curves (ASTM D86) for blends of CARBOB with ethanol.